Annals of Microbiology (2018) 68:409–418
https://doi.org/10.1007/s13213-018-1347-x

ORIGINAL ARTICLE

Deciphering the mode of action, structural and biochemical analysis of heparinase II/III (*Ps*PL12a) a new member of family 12 polysaccharide lyase from *Pseudopedobacter saltans*

Karthika Balasubramaniam[1] · Kedar Sharma[1] · Aruna Rani[1] · Vikky Rajulapati[1] · Arun Goyal[1]

Received: 19 December 2017 / Accepted: 8 May 2018 / Published online: 17 May 2018

Abstract

Heparinases are widely used for production of clinically and therapeutically important bioactive oligosaccharides and in analyzing the polydisperse, heterogeneous, and complex structures of heparin/heparan sulfate. In the present study, the gene (1911 bp) encoding heparinase II/III of family 12 polysaccharide lyase (*Ps*PL12a) from *Pseudopedobacter saltans* was cloned, expressed, and biochemically and functionally characterized. The purified enzyme *Ps*PL12a of molecular size approximately 76 kDa exhibited maximum activity in the temperature range 45–50 °C and at pH 6.0. *Ps*PL12a gave maximum activity at 1% (*w*/*v*) heparin under optimum conditions. The kinetic parameters, K_m and V_{max}, for *Ps*PL12a were 4.6 ± 0.5 mg/ml and 70 ± 2 U/mg, respectively. Ten millimolars of each Mg^{2+} and Mn^{2+} ions enhanced *Ps*PL12a activity by 80%, whereas Ni^{2+} inhibited by 75% and Co^{2+} by 10%, and EDTA completely inactivated the enzyme. Protein melting curve of *Ps*PL12a gave a single peak at 55 °C and 10 mM Mg^{2+} ions and shifted the peak to 60 °C. The secondary structure analysis of *Ps*PL12a by CD showed 65.12% α-helix, 11.84% β-strand, and 23.04% random coil. The degradation products of heparin by *Ps*PL12a analyzed by ESI-MS spectra displayed peaks corresponding to heparin di-, tetra-, penta-, and hexa-saccharides revealing the endolytic mode of enzyme action. Heparinase II/III (*Ps*PL12a) from *P. saltans* can be used for production of low molecular weight heparin oligosaccharides for their utilization as anticoagulants. This is the first report on heparinase cloned from *P. saltans*.

Keywords Glycosaminoglycans · Heparin · Heparinase · *Pseudopedobacter saltans*

Introduction

Glycosaminoglycan (GAGs) is group of linear heteropolysaccharides constituting recurring disaccharide units of hexosamine (D-glucosamine or D-galactosamine) and uronic acid (D-glucuronic or L-iduronic acid) (Ernst et al. 1995). Heparin and heparan sulfate (HS) are diverse anionic polysaccharides that are categorized under the family GAG. They are predominantly found in the outer cell surface and extracellular matrix of mammalian cells (Rabenstein 2002; Sarrazin et al. 2011; Shriver et al. 2012). The basic difference between heparin and heparan sulfate is in the degree and pattern of sulfation and uronic acid residue. Heparan sulfate consists of glucuronic acid linked to N-acetyl glucosamine, while heparin mainly has L-iduronic acid, a C-5 epimer of D-glucuronic acid (Sampaio et al. 2006). The level of sulfation in heparin is higher than its structural counterpart, HS, leading to its strong anionic nature (Gallagher and Turnbull 1992). Heparin is a well-known anticoagulant and has been widely used as a therapeutic agent to treat various thrombolytic disorders (Gray et al. 2012; Shriver et al. 2012). It has also been postulated that heparin, present within the secretory granules of connective tissue mast cells, serves as a defensive material against the invading pathogenic microorganisms (Lindahl et al. 1994; Olsson et al. 2000; Amin 2012). Heparan sulfate exists as proteoglycan that is attached to core proteins present in the basement membrane and animal cell surface. Consequently, heparan sulfate proteoglycans (HSPGs) interact with myriad of protein ligands, viz., growth factors, cytokines, chemokines and other signaling molecules leading to regulation of critical biological events such as cell-cell communication, cell

✉ Arun Goyal
arungoyl@iitg.ernet.in

[1] Carbohydrate Enzyme Biotechnology Laboratory, Department of Biosciences & Bioengineering, Indian Institute of Technology Guwahati, Guwahati, Assam 781039, India

adhesion, cell proliferation, angiogenesis, and pathogenesis (Dreyfuss et al. 2009; Sarrazin et al. 2011; Gasimli et al. 2012). Heparin and heparan sulfate GAGs are involved in various physiological processes; it is of great importance to decipher their structures to elucidate functional relationships. However, the structural heterogeneity and anionic nature of heparin and heparan sulfate pose a greater difficulty in analyzing their structures (Esko and Selleck 2002). Different analytical tools have been developed to sequence heparin and heparan sulfate polysaccharides in order to study their intricate structural details and variations. The polysaccharides have been fragmented either by means of chemicals such as nitrous oxide (Shively and Conrad 1976; Limtiaco et al. 2011) or GAG-degrading enzymes (Yamada and Sugahara 2003). The degraded products were analyzed and characterized by NMR, mass spectrometry, and HPLC (Doneanu et al. 2009, Shriver et al. 2012, Yates and Rudd 2016).

Heparin and HS-degrading enzymes are produced by both mammals and microorganisms. The difference between them lies in their mechanism of action on GAGs. Mammalian heparinase exerts its action on HSPGs through hydrolytic cleavage at the reducing end of uronic acid residues (Davies and Henrissat 1995; Toyoshima and Nakajima 1999; Hulett et al. 2000). In contrast, microbial heparinases selectively cleaves the α-(1 → 4) glycosidic linkage present in heparin and HS via β-elimination mechanism creating a C4-C5 double bond at nonreducing end of uronic acid residues (Linhardt et al. 1982; Garron and Cygler 2010). Bacteria produce three types of heparinases, viz., heparinase I, heparinase II, and heparinase III having different substrate specificities. Heparinase I primarily cleaves highly sulfated heparin, whereas heparinase III act on less sulfated heparan sulfate (Desai et al. 1993). On the contrary, heparinase II exhibits a broad specificity acting on both heparin and heparan sulfate (Linhardt et al. 1990). The three types of microbial heparinases act on heparin and HS in a specific manner; therefore, the enzymes hold great promise for decoding the complex structures of substrates. These enzymes can also be exploited for the production of low molecular weight heparin, an efficient anticoagulant having less side effects than unfractionated heparin. Furthermore, oligosaccharides that are derived from heparin and HS are known to inhibit angiogenesis and pathological disease progression (Chen et al. 1997; Lundin et al. 2000). Therefore, production of this enzyme using recombinant DNA technology and its characterization for biochemical and functional properties will lead to its use in the therapeutic field. In the present study, the gene encoding heparinase II/III, a family 12 polysaccharide lyase (*Ps*PL12a) from *Pseudopedobacter saltans* (previously classified as *Pedobacter saltans*) (Cao et al. 2014), was cloned, expressed, and purified. The biochemical, structural, and functional properties of *Ps*PL12a were studied.

Materials and methods

Bacterial strains, vectors, and substrates

The genomic DNA of *P. saltans* was obtained from DSMZ (Leibniz Institute DSMZ-German Collection of Microorganisms and Cell Cultures, Germany). The *E. coli* TOP10 and BL21 (DE3) cells used as hosts for cloning and expression, respectively, were procured from Novagen (Madison, WI). The expression vector pET28a(+) from Novagen was employed for cloning and expression. Heparin sodium salt was procured from Himedia Laboratories Pvt. Ltd., India.

Sequence analysis of *Ps*PL12a

The protein sequence of heparinase II/III of family 12 polysaccharide lyase from *P. saltans* was identified using sequencing information available at NCBI database. The gene sequence with locus tag Pedsa_1818, having GenBank accession no. ADY52373.1, encoding *Ps*PL12a from *P. saltans* was retrieved from NCBI. BLAST analysis of Pedsa_1818 was performed against UniProtKB/Swiss-Prot database to identify the homologous proteins. *Ps*PL12a conserved structural domain was determined using NCBI-Conserved Domains Database search. The protein localization of *Ps*PL12a was predicted using SignalP 4.1 server (http://www.cbs.dtu.dk/services/SignalP/). Multiple sequence alignment (MSA) of *Ps*PL12a with other homologous proteins was performed using ClustalW program. Phylogenetic relationship of *Ps*PL12a with other homologous proteins was deduced using the neighbor-joining method with Molecular Evolutionary Genetics Analysis (MEGA6) software (Kumar et al. 2016).

Gene cloning and amplification of *Ps*PL12a

The gene (1911 bp excluding the signal sequence) encoding *Ps*PL12a from *P. saltans* GenBank accession number ADY52373.1 was amplified by PCR using specific oligonucleotide primers containing *Nhe*I and *Xho*I restriction sites. The primers used for amplification were forward primer 5′-CGCGGCTAGCAAAGGTAAATCGTCCTTATC-3′ and reverse primer 5′-GCGCCTCGAGTTAAAACTGATGCTTAATAGTC-3′. The 50 μl PCR reaction mixture contained 0.45 μM of each primer (Eurofins, Luxembourg), 200 μM dNTPs (Bioline, UK), 0.025 U/μL of Taq DNA polymerase (New England Biolabs, USA), Taq DNA polymerase buffer 10× (New England Biolabs, USA), genomic DNA (15 ng), and nuclease-free water (Sigma-Aldrich Chemical Co., USA). The PCR conditions followed were initial denaturation at 94 °C for 4 min followed by 30 cycles of denaturation at 94 °C for 30 s, annealing temperature at 61 °C for 40 s, extension at 68 °C for 2 min, and final extension at 68 °C for

10 min on thermal cycler (TAKARA Bio, Japan). The amplified PCR product was run on 0.8% (*w*/*v*) agarose gel. The PCR amplified product was excised and eluted from the gel using GenElute kit (Sigma Chemical Company, USA). The purified PCR product and pET28a(+) expression vector were subjected to restriction digestion using *Nhe*I and *Xho*I (New England Biolabs, USA). T4 DNA ligase (Promega, USA) was used to ligate the restriction enzyme digested PCR fragment encoding *Ps*PL12a and pET28a(+) vector. The ligation mixture incubated in water bath (Grant, UK) at 16 °C for 16 h was used for the transformation of *E. coli* TOP10 cells. The transformed cells were spread onto LB agar plate supplemented with kanamycin (50 μg/ml) and incubated at 37 °C for 12 h. The positive clones were screened and confirmed by restriction digestion method.

Protein expression and purification of *Ps*PL12a

E. coli BL21 (DE3) cells harboring pET28a(+) containing gene encoding *Ps*PL12a were grown in 100 ml LB medium containing kanamycin (50 μg/ml). The cells were grown at 37 °C until the OD reached ~0.6 at 550 nm, followed by induction with 1 mM isopropyl β-D-1-thiogalactopyranoside (IPTG). After that, the culture was incubated at 16 °C with shaking at 180 rpm. The cells were then pelleted by centrifugation at 8000*g* for 10 min. The cell pellet was suspended in lysis buffer containing 50 mM Tris-HCl and 300 mM NaCl, pH 7.5. The suspended cells placed on ice were disrupted using sonicator (Sonics, vibra cells) with 10 s on and 15 s off pulse at 33% amplitude. The sonicated sample was centrifuged at 16,000*g* and 4 °C for 30 min to obtain the cell free extract. *Ps*PL12a containing His_6 tag was purified in a single step using immobilized metal ion affinity chromatography (IMAC). The cell-free supernatant filtered through 0.45-mm membrane was loaded onto a 1 ml Hi-Trap chelating column (GE Healthcare, USA). The column was washed with buffer containing 50 mM Tris-HCl, 300 mM NaCl, and 50 mM Imidazole, pH 7.5. *Ps*PL12a tethered to the column was eluted with elution buffer (50 mM Tris-HCl, 300 mM NaCl and 300 mM Imidazole, pH 7.5). The purity and molecular mass of recombinant *Ps*PL12a was checked on SDS-PAGE (12%, *w*/*v*). The concentration of purified *Ps*PL12a was estimated by Bradford (Bradford 1976) and UV methods using the molar extinction coefficient 141,640 M^{-1} cm^{-1} (for *Ps*PL12a) that was calculated by using Protparam tool. BSA was used as standard for Bradford assay.

Enzyme activity assay

*Ps*PL12a activity was determined by measuring the absorbance of degraded products of heparin at 232 nm by using UV-visible spectrophotometer (Varian, Cary 100, USA). The assay was performed by incubating 10 μl (1 μg/ml) of *Ps*PL12a in 50 mM sodium phosphate buffer, pH 6, containing 10 mg/ml heparin in a total reaction volume of 1 ml. The initial rate of reaction was monitored directly on a UV-visible spectrophotometer (Varian, Cary 100, USA) for 1 min by maintaining the temperature of the reaction mixture at optimum temperature, 50 °C. One international unit of enzyme activity is defined as 1 μmol of Δ4,5-uronic acid formed per minute based on a molar extinction coefficient of 5100 M^{-1} cm^{-1} at wavelength of 232 nm (Böhmer et al. 1990).

Biochemical characterization of *Ps*PL12a

The reaction conditions suitable for the enzyme activity against the substrate heparin were investigated. The optimal temperature for the activity of *Ps*PL12a was determined by incubating 990 μl of 50 mM Tris-HCl buffer (pH 7.5) containing (0.1%, *w*/*v*) heparin at different temperatures within the range of 20 to 65 °C for 5 min in a temperature-controlled spectrophotometer (Varian, Cary 100, USA). The reaction was then initiated by adding 10 μl (1 μg/ml) of enzyme *Ps*PL12a to the incubated substrate, and the reaction was monitored for 1 min. The enzyme activity was calculated as described in the "Protein expression and purification of *Ps*PL12a" section. The temperature stability of *Ps*PL12a was investigated by incubating 100 μl (100 μg/ml) of *Ps*PL12a in 50 mM sodium phosphate buffer, pH 6.0, for 1 h at temperatures varying between 30 and 60 °C. Then, 10 μl (1 μg/ml) of the enzyme was assayed in 1 ml reaction mixture for its residual activity. The pH suitable for its maximum activity was determined by using different buffer systems, viz., 50 mM citrate phosphate (pH 4–7), 50 mM sodium phosphate (pH 6–8), and 50 mM Tris-HCl (pH 8–9). The activity of *Ps*PL12a was monitored by recording the absorbance at 232 nm (A_{232}) for 1 min using UV-visible spectrophotometer (Varian, Cary 100), maintaining the temperature at 50 °C. For determination of pH stability, 100 μl (0.1 mg/ml) of *Ps*PL12a was incubated at various pH using 50 mM citrate phosphate (pH 4–7), 50 mM sodium phosphate (pH 6–8), 50 mM Tris-HCl (pH 8–9), and 50 mM glycine-NaOH at 25 °C for 1 h. Ten microliters of *Ps*PL12a was withdrawn and added to 990 μl 50 mM sodium phosphate buffer, pH 6.0, containing 10 mg/ml (1%, *w*/*v*) heparin, and its residual activity was determined at 50 °C.

Determination of kinetic parameters of *Ps*PL12a

The *Ps*PL12a activity was measured against heparin by varying its concentration from 0.01% (*w*/*v*) to 1.6% (*w*/*v*). The kinetic parameters were determined by plotting the initial rate of reaction as a function of substrate concentration. The enzyme reaction was monitored on UV-visible spectrophotometer at A_{232} for 1 min under optimum conditions of temperature

50 °C and pH 6.0. The absorbance recorded was converted to units based on molar extinction coefficient (ε) of 5100 M^{-1} cm^{-1} (Böhmer et al. 1990). The kinetic parameters were determined by using GraphPad Prism v6.03 software.

Effect of metal ions on *Ps*PL12a activity

The effect of NaCl, $MgCl_2$, $MnCl_2$, $CaCl_2$, $CoCl_2$, and $NiSO_4$ containing metal ions namely Na^+, Mg^{2+}, Mn^{2+}, Ca^{2+}, Co^{2+}, and Ni^{2+}, respectively, and EDTA on the activity of *Ps*PL12a enzyme was investigated. In order to avoid precipitation, all the metal ions were dissolved in 50 mM MES buffer at optimum pH 6. The concentration of metal ions and EDTA ranging from 0.5 to 20 mM and for NaCl from 10 to 600 mM were used and incubated in 990 μl of heparin (1%, *w*/*v*) in 50 mM MES buffer, pH 6.0, at 50 °C. The absorbance, A_{232}, was recorded after adding 10 μl (100 μg/ml) of enzyme to above 990 μl substrate solution for 1 min. The relative activity of *Ps*PL12a was expressed as percent of activity with respect to the control (without the addition of metal ions), taking as 100%.

Protein melting curve of *Ps*PL12a

The melting profile of *Ps*PL12a was generated by exposing the protein to different temperatures ranging from 20 to 100 °C using UV-visible spectrophotometer coupled with peltier temperature controller (Varian, Cary 100, USA). The change in absorbance of protein was recorded at 280 nm, and the protein was held at each temperature for 2 min. The 1 ml of purified *Ps*PL12a (50 μg/ml) suspended in 50 mM MES buffer, pH 6.0, was used. The experiment was also carried out in the presence of 10 mM Ca^{2+}or 10 mM Mg^{2+} ions in 1 ml protein (50 μg/ml) solution. MES buffer was used in order to avoid precipitation of metal ions as stated earlier. The melting curve of *Ps*PL12a was obtained by plotting change in absorbance at 280 nm versus temperature.

CD analysis of *Ps*PL12a

The compositions of secondary structural elements were determined by circular dichroism (CD) spectroscopy. Purified *Ps*PL12a (0.7 mg/ml) dissolved in 50 mM Tris-HCl, pH 7.5, was analyzed in the far UV region (190–250 nm) using CD. The CD spectrum for *Ps*PL12a was recorded using a sample cell with path length 0.1 cm on a spectro-polarimeter (Jasco Corporation, J-815, Japan) at 25 °C. The CD spectrum was plotted as a function of wavelength and mean residual ellipticity (MRE deg cm^{-1} M^{-1}). Buffer contributions were corrected, and the secondary structures were determined using K2D3 server.

ESI-mass spectrometric analysis of *Ps*PL12a degraded products of heparin

The reaction of *Ps*PL12a and heparin was set up at optimized conditions of the enzyme to generate degradation products of heparin. Ten microliters of purified *Ps*PL12a (10 μg/ml, 52 U/mg) was added in 1 ml of 10 mg/ml heparin dissolved in 50 mM sodium phosphate buffer, pH 6.0, and incubated at 37 °C for 5 min, 30 min, and 12 h. The reaction was terminated by adding equal volume of absolute ethanol (1 ml) to 1 ml reaction mixture. The undigested polysaccharide was removed by centrifuging the reaction mixture at 13,000*g* at 25 °C for 10 min. The supernatant containing the heparin oligosaccharides were then concentrated to 150 μl at 70 °C in hot air oven. Subsequently, the concentrated samples were diluted in 1:1 (*v*/*v*) ratio by methanol, and 30 μl was used for further investigation. The electron spray ionization (ESI) mass spectra of the degraded products of heparin by *Ps*PL12a after 5 min, 30 min, and 24 h were obtained by ESI mass spectrometer (Waters, Q-TOF Premier). ESI-MS analysis was performed in negative ion mode, and the conditions followed were as follows: capillary voltage 3 eV, collision energy 5 eV, ionization energy 1 eV, desolvation temperature 250 °C, and the source temperature of 80 °C.

Results and discussion

Sequence analysis of *Ps*PL12a from *P. saltans*

The analysis of the whole genome sequence of *P. saltans* confirmed the presence of two family 12 polysaccharide lyases (GenBank accession numbers ADY52369.1 and ADY52373.1). The selected gene encoding heparinase II/III (GenBank accession number ADY52373.1) displayed high sequence similarity with previously characterized heparinase II/III from other organisms. BLAST analysis of amino acid sequence of *Ps*PL12a (Pedsa_1818) revealed the presence of putative heparinase II/III. The protein localization prediction of *Ps*PL12a gave an insight of the presence of long N-terminal signal peptide consisting of 19 amino acid residues with a cleavage site between Gly19 and Lys20 using SignalP 4.1 server (http://www.cbs.dtu.dk/services/SignalP/). The putative heparinase II/III activity showed catalytic domain at C-terminal spanning from 20 to 655 amino acids (Fig. 1a). BLAST analysis of *Ps*PL12a showed 55% sequence homology, with heparinase II/III from *Pedobacter heparinus* (UniProt ID: Q59289.1), 49% similarity with heparinase II/III from *Bacteroides stercoris* (UniProt ID: C7EXL6.1), and 31% with heparinase II/III from *Bacteroides thetaiotaomicron* (UniProt ID: Q89YR9.1). The phylogenetic tree analysis also showed similar results where *Ps*PL12a, clustered under the homologus

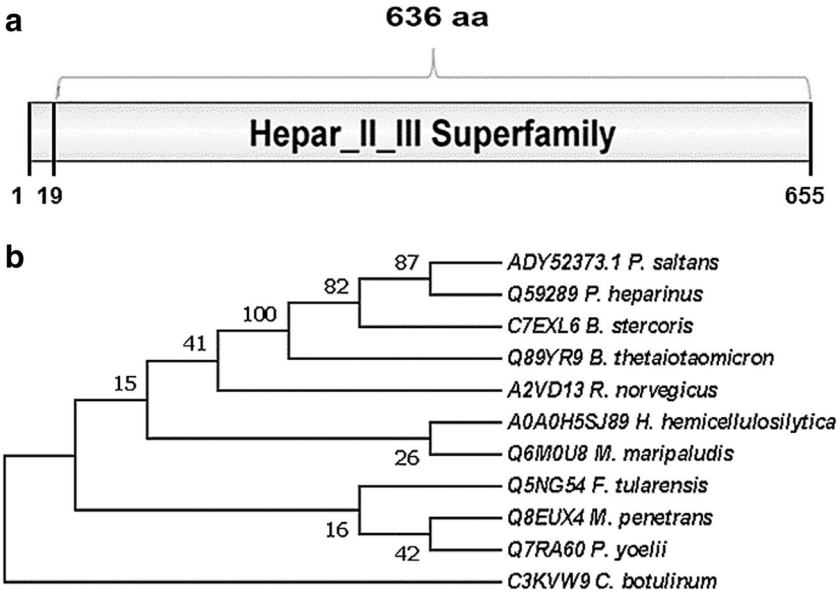

Fig. 1 **a** Molecular architecture of *Ps*PL12a showing an N-terminal signal peptide followed by catalytic domain having putative heparinase activity. **b** The phylogenetic tree showing the comparative analysis of *Ps*PL12a with homologous heparinases (Uniprot IDs: Q59289, C7EXL6, Q89YR9) and other enzymes (Uniprot IDs: A2VD13, A0A0H5SJ89, Q6M0U8, Q5NG54, Q8EUX4, Q7RA60, C3KVW9) from different origins

heparinases from *Pedobacter heparinus*, *B. stercoris*, and *Bacteroides thetaiotaomicron* (Fig. 1b).

Cloning, expression, and purification of *Ps*PL12a

The gene (1911 bp) encoding *Ps*PL12a was amplified and ligated to pET28a(+) vector as described in the "Materials and methods" section. The recombinant plasmid was isolated from *E. coli* TOP 10 cells and transformed into *E. coli* BL21 (DE3) cells for the expression of *Ps*PL12a protein. The expressed recombinant protein *Ps*PL12a possessing N-terminal His6-tag was purified by immobilized metal ion affinity chromatography. The SDS-PAGE (12%, *w*/*v*) analysis of purified enzyme displayed a single band of molecular size, approximately 76 kDa, which was also similar to the theoretical size predicted by protparam (76.53 kDa) (Fig. 2). The purified protein (*Ps*PL12a) was used for further enzyme activity studies.

Biochemical characterization of *Ps*PL12a

The optimum temperature for the maximum activity of *Ps*PL12a was 50 °C (Fig. 3a). *Ps*PL12a retained around 90% of activity at 40 °C. The activity of the enzyme decreased above 50 °C and was completely lost at 65 °C (Fig. 3a). The temperature tolerance of the enzyme was studied by incubating the enzyme at different temperature for a period of 1 h. *Ps*PL12a was stable within the temperature range 30 to 40 °C (Fig. 3b). However, the enzyme lost 80% of its activity at 45 °C when incubated for 1 h, though the optimum temperature of *Ps*PL12a was in the range 45 to 50 °C. This may be attributed to the mesophilic nature of *P. saltans*. Maximum activity of *Ps*P12a was found to be at pH 6 in 50 mM sodium phosphate/citrate phosphate buffer. The activity rapidly decreased above pH 6.5 and was completely lost at pH 9 (Fig. 3c). *Ps*PL12a was stable within the pH range 6–9 for 1 h under respective buffers as shown in Fig. 3d. *Ps*PL12a showed optimum temperature of 50 °C and pH 6 in 50 mM sodium phosphate/citrate phosphate buffer. Previously reported heparinase from *B. stercoris* showed optimum pH 6.6 and temperature 45 °C with heparan sulfate as substrate (Hyun et al. 2010). It has been reported that heparinase from various organisms have optimum pH within the range 6.6–7.8 and optmimum temperature between 30 and 45 °C (Hovingh and Linker 1970; Nader et al. 1990; Chen et al. 2011). However, this is the first report on heparinase from *P. saltans* showing maximum activity at optimum pH 6.0 and at the temperature 50 °C.

Determination of kinetic parameters of *Ps*PL12a

The kinetic parameters of *Ps*PL12a were determined from Michaelis-Menten plot. The enzyme displayed K_m 4.6 ± 0.5 mg/ml and V_{max} 70 ± 2 U/mg with heparin as a substrate. The turnover number (k_{cat}) and catalytic efficiency (k_{cat}/K_m) of *Ps*PL12a were found to be 89 s^{-1} and 19.3 s^{-1} mg^{-1} ml, respectively.

Effect of metal ions on the activity of *Ps*PL12a

The effect of various metal ions, viz., Mg^{2+}, Mn^{2+}, Ca^{2+}, Co^{2+}, Ni^{2+}, and EDTA on the activity of *Ps*PL12a was investigated. *Ps*PL12a activity was enhanced by the addition of Mg^{2+}, Mn^{2+}, or Ca^{2+} divalent cations (Fig. 4a–c and Table 1). The enzyme activity increased by 80% with addition of 10 mM Mg^{2+} or 10 mM Mn^{2+} ions and increased only 25% by 10 mM Ca^{2+}. The enzyme activity was adversely affected by Co^{2+} and Ni^{2+} ions. Ten millimolars Ni^{2+} inhibited by 75% (Fig. 4d) and Co^{2+} ion inhibited by 10%. The residual activity of *Ps*PL12a was drastically decreased up to 5% by 10 mM EDTA (Fig. 4e), suggesting the role of divalent cations

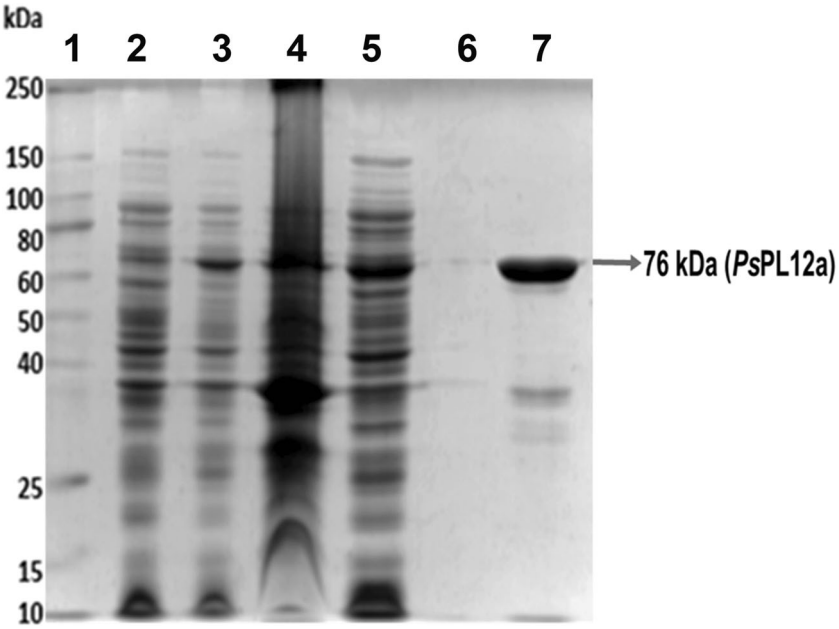

Fig. 2 SDS-PAGE (12%, *w*/*v*) showing single protein band of size, 76 kDa, of *Ps*PL12a; lane 1: protein ladder (250 kDa); lane 2: uninduced cells BL21 (DE3); lane 3: induced cells BL21 (DE3); lane 4: cell pellet after sonication; lane 5: cell-free extract; lane 6: last wash from column; lane 7: purified protein (76 kDa)

in its catalytic activity (Table 1). The activity of heparinase II from *Bacillus circulans* (Yoshida et al. 2002), *Bacillus* sp. FERM BP2613 (Bellamy and Horikoshi 1992), and heparinase III from *B. stercoris* HJ-15 NCB146506 (Kim et al., 2000) was also enhanced by Mg^{2+} and Ca^{2+} ions. However, the activity of heparinase II from *Pedobacter*

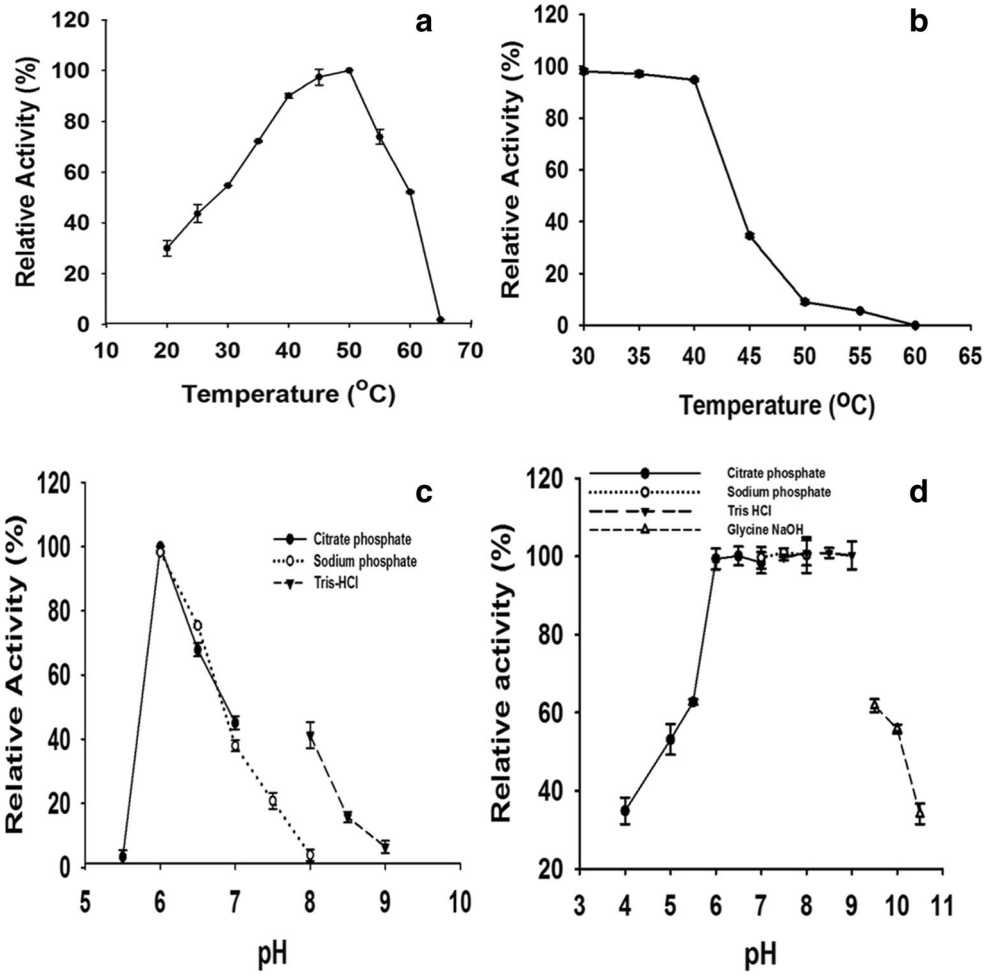

Fig. 3 **a** Effect of temperature on the activity of *Ps*PL12a. The activity of enzyme at 50 °C was taken as 100%. **b** Temperature stability profile of *Ps*PL12a. The residual activity was measured after 1-h incubation of the enzyme (*Ps*PL12a) at different temperatures. **c** Plot showing the effect of pH on the activity of *Ps*PL12a. **d** Study on stability of *Ps*PL12a at various pH. The enzyme activity was measured after 60-min incubation at different pH using appropriate buffer. All the experiments were performed in triplicate ($n = 3$). The error bar represents the standard deviation

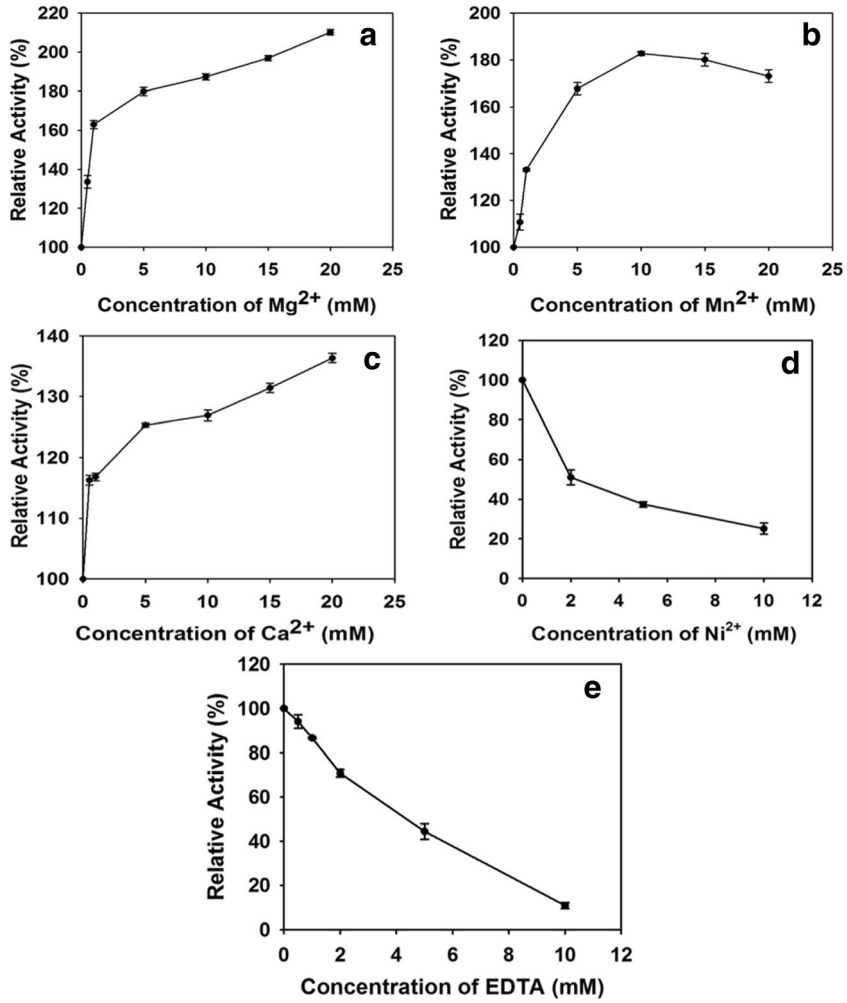

Fig. 4 Plot showing effect of different metal ions on *Ps*PL12a activity. **a** Effect of Mg^{2+} on the activity of *Ps*PL12a. **b** Plot showing effect of Mn^{2+} on the activity of *Ps*PL12a. **c** Ca^{2+} effect on the activity of *Ps*PL12a. **d**, **e** Plots showing inhibitory effects of Ni^{2+} and EDTA. All the experiments were performed in triplicate ($n = 3$). The error bar represents the standard deviation

heparinus was inhibited by Ca^{2+} ions (Lohse and Linhardt 1992; Steyn et al. 1998). The activity of *Ps*PL12a increased by 18% in presence of 50 mM NaCl, and beyond this concentration, the activity decreased. The similar effect of NaCl was reported for activity of heparin lyase I and heparin lyase III from *Pedobacter heparinus* (Lohse and Linhardt 1992). Whereas, heparinase III from *B. stercoris* HJ-15 showed no activity in the absence of NaCl, but its activity was

Table 1 Effect of metal ions on activity of *Ps*PL12a using heparin as substrate

Metal ion	Concentration (mM)	Relative activity (%)
Control	–	100
Mg^{2+}	10	186 ± 0.7
Mn^{2+}	10	180 ± 0.8
Ca^{2+}	10	124 ± 0.9
Na^{+}	50	118 ± 1.8
Co^{2+}	10	90 ± 1.2
Ni^{2+}	10	25 ± 3.0
EDTA	10	5.5 ± 1.3

All experiments were performed in triplicate ($n = 3$). The values represented are mean ± standard deviation

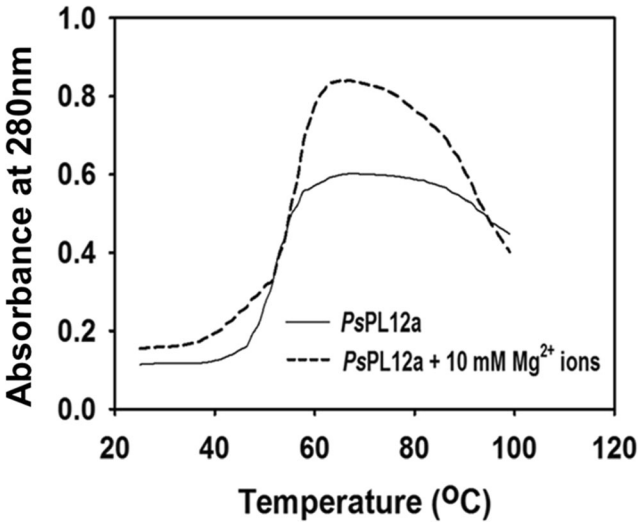

Fig. 5 Melting profile of *Ps*PL12a without any additive and in the presence of 10 mM Mg^{2+} ions

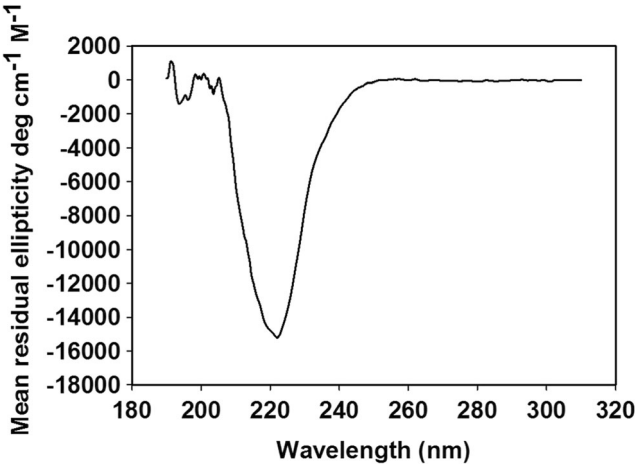

Fig. 6 CD spectrum of *Ps*PL12a in far UV region

significantly enhanced by 32-fold against heparin, on the addition of 350 mM NaCl (Hyun et al. 2010).

Protein melting curve of *Ps*PL12a

A single melting peak was observed at 55 °C for *Ps*PL12a (Fig. 5). There was a shift in its metling peak towards higher temperature to 60 °C with the addition of 10 mM Mg^{2+} ions (Fig. 5). There was no shift in the peak when 10 mM Ca^{2+} was added to *Ps*PL12a. The results showed that Mg^{2+} ions prevented thermal denaturation of protein. Mg^{2+} ions play an important role in enhancing both the enzyme activity and thermal stability of *Ps*PL12a.

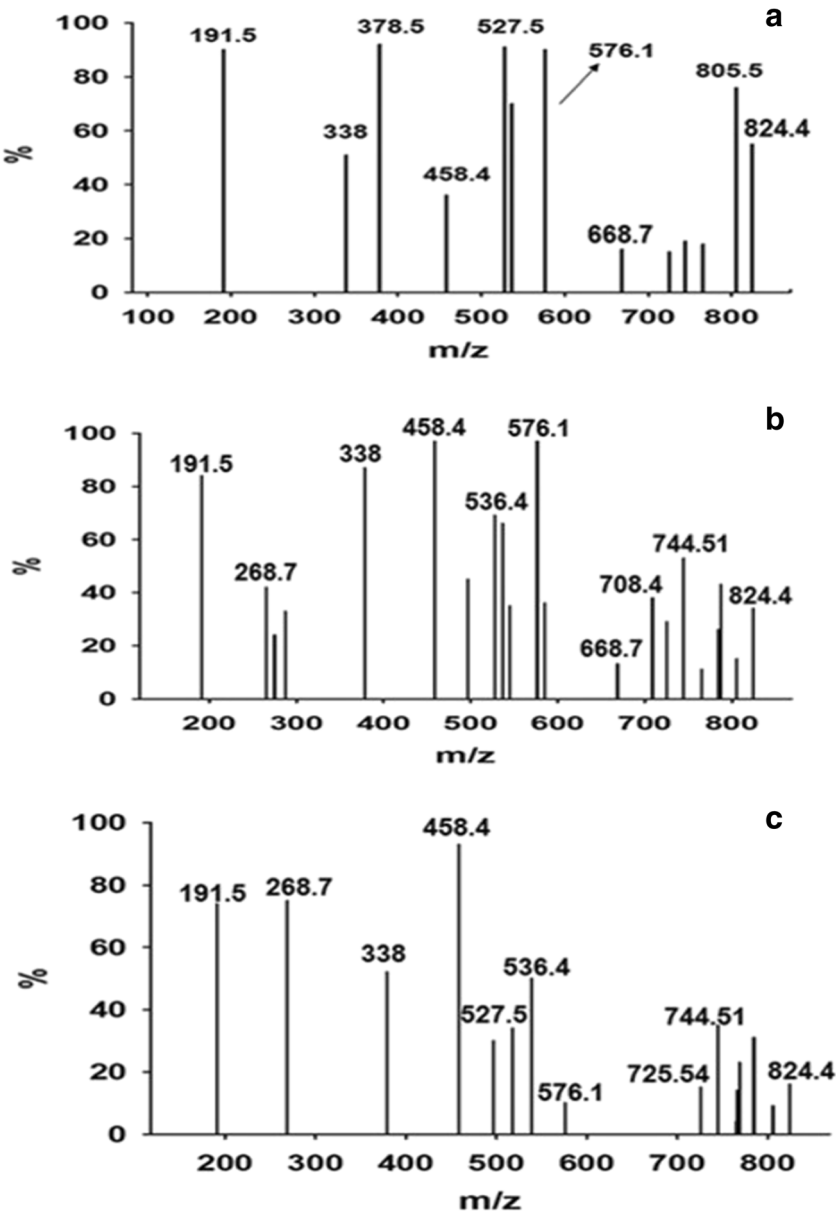

Fig. 7 ESI-MS spectra of *Ps*PL12a degraded products of heparin. MS analysis of **a** 5 min, **b** 30 min, and **c** 12 h samples

Secondary structure analysis of *Ps*PL12a by CD

The data obtained after cicrlular dichroism (CD) analysis of *Ps*PL12a were further analyzed using K2D3 software. The CD results revealed the presence of 65.12% α-helices, 11.84% β-strands, and 23.04% random coils in *Ps*PL12a structure (Fig. 6).

ESI-mass spectrometric analysis of degraded products of heparin by *Ps*PL12a

*Ps*PL12a degraded heparin products obtained at 5 min, 30 min, and 12 h were analyzed by ESI-MS. The ESI-MS spectrum of 5 min sample showed peaks corresponding to triply charged tri-sulfated disaccharide (ΔUA2S-GlcNS6S) with *m/z* 191.5; singly charged nonsulfated disaccharide (ΔUA-GlcN) with *m/z* 338; mono-acetylated singly charged disaccharide (ΔUA-GlcNAc) with *m/z* 378.5; mono-sulfated, mono-acetylated singly charged disaccharide (ΔUA-GlcNAc6S) with *m/z* 458.4; tetra-sulfated, mono-acetylated doubly charged tetra-saccharide having *m/z* 527.5; and hexa-sulfated (ΔUA2S-GlcNS6S-IdoA2S-GlcNS6S) doubly charged having *m/z* 576.1 (Fig. 7a). The ESI-MS spectrum also displayed the peaks corresponding to higher oligosaccharides, viz., doubly charged penta-saccharide with *m/z* 668.7; hepta-sulfated, mono-acetylated doubly charged hexa-saccharide (ΔUA2S-GlcNS6S-IdoA-GlcNAc6S-GlcA-GlcNS3S6S) with *m/z* 805.49; and octa-sulfated doubly charged hexa-saccharide (ΔUA2S-GlcNS6S-IdoA2S-GlcNS6S-GlcA-GlcNS6S) with *m/z* 824.47 (Fig. 7a). The ESI-MS spectra for 30 min and 12 h samples also showed peaks corresponding to di-, tetra-, penta-, and hexa-saccharide of heparin, suggesting a random endolytic mode of action by *Ps*PL12a (Fig. 7b, c). The peak intensities of higher oligosaccharides, i.e., hepta-sulfated doubly charged hexa-saccharide (ΔUA2S-GlcNS6S-IdoA-GlcNAc6S-GlcA-GlcNS3S6S) with *m/z* 805.49 and octa-sulfated doubly charged hexa-saccharide (ΔUA2S-GlcNS6S-IdoA2S-GlcNS6S-GlcA-GlcNS6S) with *m/z* 824.47, reduced with increase in the reaction time from 5 min to 12 h (Fig. 7a–c). The *m/z* values of heparin oligosaccharide peaks were assigned based on the previous ESI-MS reports (Thanawiroon et al. 2004; Saad et al. 2005; Xiao et al. 2010).

Conclusion

A new member (*Ps*PL12a) of family 12 polysaccharide lyase (PL12) from *P. saltans* was cloned, expressed, and purfied as a homogeneous protein of molecular size approximately 76 kDa. *Ps*PL12a showed activity against the substrate heparin with V_{max} 70 ± 2 U/mg, K_m 4.6 ± 0.5 mg/ml, k_{cat} 89 s^{-1}, and $k_{cat/km}$ 19.3 s^{-1} mg^{-1} ml. The enzyme displayed an optimum temperature of 50 °C and pH 6 in 50 mM sodium phosphate/citrate phosphate buffer. Mg^{2+} ions played an important role by enhancing the enzyme activity as well as imparting thermostability to *Ps*PL12a. ESI-MS analysis of heparin-degraded products by *Ps*PL12a revealed its endolytic mode of cleavage. *Ps*PL12a displaying affinity for the substrate heparin can be exploited for the production of low molecular weight heparin that has several therapeutic applications. It has been reported that heparinase and its degradation products inhibit angiogenesis and disease progression. Hence, *Ps*PL12a can be used to explore the structural features of heparin and heparan sulfate glycosaminoglycans involved in the regulation of important biological process inlcuding angiogenesis, disease progression, and cell-cell interactions. Further, structural analysis of the enzyme would shed light on its catalytic mechanism leading to better understanding of its controlled usage, in order to produce therapeutically important heparin oligosaccharides.

Acknowledgements The authors thank DBT Program Support, IIT Guwahati, for CD analysis and Central Instrumentation Facility for ESI-mass analysis. Fellowship provided by the Ministry of Human Resource Development, Govt. of India, to Karthika B. is gratefully acknowledged.

Compliance with ethical standards

Conflict of interest The authors declare that they have no conflict of interest.

References

Amin K (2012) The role of mast cells in allergic inflammation. Respir Med 106(1):9–14

Bellamy RW, Horikoshi K (1992) U.S. patent no. 5,145,778. U.S. Patent and Trademark Office, Washington, DC

Böhmer LH, Pitout MJ, Steyn PL, Visser L (1990) Purification and characterization of a novel heparinase. J Biol Chem 265(23):13609–13617

Bradford MM (1976) A rapid and sensitive method for the quantitation of microgram quantities of protein utilizing the principle of protein-dye binding. Anal Biochem 72(1–2):248–254

Cao J, Lai Q, Li G, Shao Z (2014) *Pseudopedobacter beijingensis* gen. nov., sp. nov., isolated from coking wastewater activated sludge, and reclassification of *Pedobacter saltans* as *Pseudopedobacter saltans* comb. nov. Int J Syst Evol Microbiol 64(6):1853–1858

Chen Y, Maguire T, Hileman RE, Fromm JR, Esko JD, Linhardt RJ, Marks RM (1997) Dengue virus infectivity depends on envelope protein binding to target cell heparan sulfate. Nat Med 3(8):866–871

Chen S, Ye F, Chen Y, Chen Y, Zhao H, Yatsunami R, Nakamura S, Arisaka F, Xing XH (2011) Biochemical analysis and kinetic modeling of the thermal inactivation of MBP-fused heparinase I: implications for a comprehensive thermostabilization strategy. Biotechnol Bioeng 108(8):1841–1851

Davies G, Henrissat B (1995) Structures and mechanisms of glycosyl hydrolases. Structure 3(9):853–859

Desai UR, Wang HM, Linhardt RJ (1993) Specificity studies on the heparin lyases from *Flavobacterium heparinum*. Biochemistry 32(32):8140–8145

Doneanu CE, Chen W, Gebler JC (2009) Analysis of oligosaccharides derived from heparin by ion-pair reversed-phase chromatography/mass spectrometry. Anal Chem 81(9):3485–3499

Dreyfuss JL, Regatieri CV, Jarrouge TR, Cavalheiro RP, Sampaio LO, Nader HB (2009) Heparan sulfate proteoglycans: structure, protein interactions and cell signaling. An Acad Bras Cienc 81(3):409–429

Ernst S, Langer R, Cooney CL, Sasisekharan R (1995) Enzymatic degradation of glycosaminoglycans. Crit Rev Biochem Mol Biol 30(5): 387–444

Esko JD, Selleck SB (2002) Order out of chaos: assembly of ligand binding sites in heparan sulfate. Annu Rev Biochem 71(1):435–471

Gallagher JT, Turnbull JE (1992) Heparan sulphate in the binding and activation of basic fibroblast growth factor. Glycobiology 2(6):523–528

Garron ML, Cygler M (2010) Structural and mechanistic classification of uronic acid-containing polysaccharide lyases. Glycobiology 20(12): 1547–1573

Gasimli L, Robert JL, Dordick JS (2012) Proteoglycans in stem cells. Biotechnol Appl Biochem 59(2):65–76

Gray E, Hogwood J, Mulloy B (2012) The anticoagulant and antithrombotic mechanisms of heparin. In: Heparin-A century of Progress. Springer, Berlin Heidelberg, pp 43–61

Hovingh P, Linker A (1970) The enzymatic degradation of heparin and heparitin sulfate III. Purification of a heparitinase and a heparinase from *flavobacteria*. J Biol Chem 245(22):6170–6175

Hulett MD, Hornby JR, Ohms SJ, Zuegg J, Freeman C, Gready JE, Parish CR (2000) Identification of active-site residues of the pro-metastatic endoglycosidase heparanase. Biochemistry 39(51):15659–15667

Hyun YJ, Lee JH, Kim DH (2010) Cloning, overexpression, and characterization of recombinant heparinase III from *Bacteroides stercoris* HJ-15. Appl Microbiol Biotechnol 86(3):879–890

Kumar S, Stecher G, Tamura K (2016) MEGA7: molecular evolutionary genetics analysis version 7.0 for bigger datasets. Mol Biol Evol 33(7):1870–1874

Limtiaco JF, Beni S, Jones CJ, Langeslay DJ, Larive CK (2011) NMR methods to monitor the enzymatic depolymerization of heparin. Anal Bioanal Chem 399(2):593–603

Lindahl U, Lidholt K, Spillmann D, Kjellén L (1994) More to "heparin" than anticoagulation. Thromb Res 75(1):1–32

Linhardt RJ, Fitzgerald GL, Cooney CL, Langer R (1982) Mode of action of heparin lyase on heparin. Biochim Biophys Acta Protein Struct Mol Enzymol 702(2):197–203

Linhardt RJ, Turnbull JE, Wang HM, Loganathan D, Gallagher JT (1990) Examination of the substrate specificity of heparin and heparan sulfate lyases. Biochemistry 29(10):2611–2617

Lohse DL, Linhardt RJ (1992) Purification and characterization of heparin lyases from Flavobacterium heparinum. J Biol Chem 267(34): 24347–24355

Lundin L, Larsson H, Kreuger J, Kanda S, Lindahl U, Salmivirta M, Claesson-Welsh L (2000) Selectively desulfated heparin inhibits fibroblast growth factor-induced mitogenicity and angiogenesis. J Biol Chem 275(32):24653–24660

Nader HB, Porcionatto MA, Tersariol IL, Pinhal MA, Oliveira FW, Moraes CT, Dietrich CP (1990) Purification and substrate specificity of heparitinase I and heparitinase II from *Flavobacterium heparinum*. Analyses of the heparin and heparan sulfate degradation products by 13C NMR spectroscopy. J Biol Chem 265(28):16807–16813

Olsson P, Sanchez J, Mollnes TE, Riesenfeld J (2000) On the blood compatibility of end-point immobilized heparin. J Biomater Sci Polym Ed 11(11):1261–1273

Rabenstein DL (2002) Heparin and heparan sulfate: structure and function. Nat Prod Rep 19(3):312–331

Saad OM, Ebel H, Uchimura K, Rosen SD, Bertozzi CR, Leary JA (2005) Compositional profiling of heparin/heparan sulfate using mass spectrometry: assay for specificity of a novel extracellular human endosulfatase. Glycobiology 15(8):818–826

Sampaio LO, Tersariol IL, Lopes CC, Bouças RI, Nascimento FD, Rocha HA, Nader HB (2006) Heparins and heparans sulfates. Structure, distribution and protein interactions. Insights into Carbohydrate Structure and Bological Function, 1–24

Sarrazin S, Lamanna WC, Esko JD (2011) Heparan sulfate proteoglycans. Cold Spring Harb Perspect Biol 3(7):a004952

Shively JE, Conrad HE (1976) Formation of anhydrosugars in the chemical depolymerization of heparin. Biochemistry 15(18):3932–3942

Shriver Z, Capila I, Venkataraman G, Sasisekharan R (2012) Heparin and heparan sulfate: analyzing structure and microheterogeneity. Heparin-A Century of Progress. Springer Berlin Heidelberg. 159–176

Steyn PL, Segers P, Vancanneyt M, Sandra P, Kersters K, Joubert JJ (1998) Classification of heparinolytic bacteria into a new genus, Pedobacter, comprising four species: *Pedobacter heparinus* comb. nov., *Pedobacter piscium* comb. nov., *Pedobacter africanus* sp. nov. and *Pedobacter saltans* sp. nov. proposal of the family Sphingobacteriaceae fam. nov. Int J Syst Evol Microbiol 48(1):165–177

Thanawiroon C, Rice KG, Toida T, Linhardt RJ (2004) Liquid chromatography/mass spectrometry sequencing approach for highly sulfated heparin-derived oligosaccharides. J Biol Chem 279(4): 2608–2615

Toyoshima M, Nakajima M (1999) Human heparanase purification, characterization, cloning, and expression. J Biol Chem 274(34):24153–24160

Xiao Z, Zhao W, Yang B, Zhang Z, Guan H, Linhardt RJ (2010) Heparinase 1 selectivity for the 3, 6-di-O-sulfo-2-deoxy-2-sulfamido-α-D-glucopyranose (1, 4) 2-O-sulfo-α-L-idopyranosyluronic acid (GlcNS3S6S-IdoA2S) linkages. Glycobiology 21(1):13–22

Yamada S, Sugahara K (2003) Preparation of oligosaccharides from sulfated glycosaminoglycans using bacterial enzymes. In: Capillary electrophoresis of carbohydrates, pp 71–78

Yates EA, Rudd TR (2016) Recent innovations in the structural analysis of heparin. Int J Cardiol 212:S5–S9

Yoshida E, Sakai K, Tokuyama S, Miyazono H, Maruyama H, Morikawa K, Tahara Y (2002) Purification and characterization of heparinase that degrades both heparin and heparan sulfate from *Bacillus circulans*. Biosci Biotechnol Biochem 66(5):1181–1184